

**Zeitschrift:** Schweizerische mineralogische und petrographische Mitteilungen =  
Bulletin suisse de minéralogie et pétrographie

**Band:** 70 (1990)

**Heft:** 3

**Artikel:** Tectonic significance of an early-Alpine P-T-deformation path from  
Austroalpine micaschists to the south of the Tauern Window, Eastern  
Alps

**Autor:** Schulz, Bernhard

**DOI:** <https://doi.org/10.5169/seals-53631>

### **Nutzungsbedingungen**

Die ETH-Bibliothek ist die Anbieterin der digitalisierten Zeitschriften auf E-Periodica. Sie besitzt keine Urheberrechte an den Zeitschriften und ist nicht verantwortlich für deren Inhalte. Die Rechte liegen in der Regel bei den Herausgebern beziehungsweise den externen Rechteinhabern. Das Veröffentlichen von Bildern in Print- und Online-Publikationen sowie auf Social Media-Kanälen oder Webseiten ist nur mit vorheriger Genehmigung der Rechteinhaber erlaubt. [Mehr erfahren](#)

### **Conditions d'utilisation**

L'ETH Library est le fournisseur des revues numérisées. Elle ne détient aucun droit d'auteur sur les revues et n'est pas responsable de leur contenu. En règle générale, les droits sont détenus par les éditeurs ou les détenteurs de droits externes. La reproduction d'images dans des publications imprimées ou en ligne ainsi que sur des canaux de médias sociaux ou des sites web n'est autorisée qu'avec l'accord préalable des détenteurs des droits. [En savoir plus](#)

### **Terms of use**

The ETH Library is the provider of the digitised journals. It does not own any copyrights to the journals and is not responsible for their content. The rights usually lie with the publishers or the external rights holders. Publishing images in print and online publications, as well as on social media channels or websites, is only permitted with the prior consent of the rights holders. [Find out more](#)

**Download PDF:** 29.04.2026

**ETH-Bibliothek Zürich, E-Periodica, <https://www.e-periodica.ch>**

# Tectonic significance of an early-Alpine P-T-deformation path from Austroalpine micaschists to the south of the Tauern Window, Eastern Alps

par Bernhard Schulz<sup>1</sup>

## Abstract

An early-Alpine P-T-deformation path was obtained from garnet-micaschists of the Alpidic Austroalpine basement by applying geothermobarometric calibrations to the deformation-related chemical evolution of minerals in incompletely preserved assemblages. A relative P-T path from temporarily syn-crystalline rotated garnets describes the prograde metamorphic evolution (increasing T, mainly decreasing P) during the generation of a foliation S2 by a simple-shear-dominated deformation D1-D2. Muscovites with different mineral chemistry in foliation S2 and a younger crenulation foliation S3 recorded a subsequent isobaric temperature decrease from 4 kb / 550 °C to 3.5 kb / 350 °C synchronous to a pure-shear-dominated deformation D3. The general shape of the P-T path is characteristic of successive understacking – overstacking – uplift – further understacking / screen effect of tectonic units in a collisional scenario. Radiometric dating by other authors suggests a pre-100 Ma age of this collision history.

*Keywords:* Microstructures, mineral chemistry, geothermobarometry, P-T-deformation path, early-Alpine collision, Eastern Alps.

## Zusammenfassung

Aus Granat-Glimmerschiefern des alpidisch überprägten ostalpinen Basements wurde ein frühalpiner P-T-Deformationspfad ermittelt. Die Anwendung der geothermobarometrischen Kalibrierungen erfolgte an Mineralen, die teilweise in unvollständiger Paragenese vorliegen und die eine chemische Entwicklung mit enger Beziehung zur Deformationsgeschichte aufweisen. Ein relativer P-T-Pfad von zeitweise synkristallin rotierten Granaten beschreibt die prograde Metamorphose (steigende Temperaturen, hauptsächlich sinkende Drücke) während der Bildung einer Foliation S2 durch Scherdeformation D1-D2. Chemisch unterschiedlich zusammengesetzte Hellglimmer in S2 und einer jüngeren Crenulationsschieferung S3 registrierten einen darauffolgenden isobaren Temperaturrückgang von 4 kb / 550 °C auf 3.5 kb / 350 °C im Verlauf einer überwiegend koaxialen Deformation D3. Die generelle Form des P-T-Pfades ist für eine aufeinanderfolgende Unterschiebung – Überschiebung – Hebung – weitere Unterschiebung / Temperatur-Abschirm-Effekt (screen effect) mehrerer tektonischer Einheiten bei einer Kontinent-Kollision kennzeichnend. Radiometrische Datierungen anderer Autoren deuten darauf hin, dass diese Kollisionsgeschichte älter als 100 Ma ist.

## 1. Introduction

The lithologic and tectonic transition between the Austroalpine basement complex (ABC) to the south and the Upper Schieferhülle (USH) of the Penninic complex to the north is considered to be the most important Alpine borderline and suture in the Eastern Alps (Fig. 1a, 1b). During an early-Alpine continental collision the pre-Alpine Austroalpine basement complex, belonging to the

Adriatic plate, has moved to the north (FRISCH, 1978; ROEDER and BÖGEL, 1978; TOLLMANN, 1987) and now overlies the pre-Alpine Central gneisses of the European continental crust which outcrops in the central Tauern Window. The crust of the Penninic ocean, initially situated between the Adriatic (Apulian) and European plates, was previously subducted beneath the Adriatic plate. Mesozoic sedimentary and magmatic rocks which had covered the Penninic oceanic crust have been

<sup>1</sup> Institut für Geologie und Mineralogie, Schlossgarten 5, D-8520 Erlangen, Federal Republic of Germany.

scraped off and are found in the Upper Schieferhülle and Matreier Zone between the continental plates. A partial subduction of the Mesozoic rocks and the Central gneisses beneath the Austroalpine basement complex is considered to be responsible for intense Alpine regional metamorphism in the Tauern Window and its frame (see below).

Early-, middle-, and late-Alpine metamorphic events at 120–80 Ma, 50–30 Ma and 20 Ma were discussed by RAITH et al. (1978), BORSI et al. (1978) and SASSI et al. (1974, 1980). The thermal condi-

tions and metamorphic isograds of the middle-Alpine metamorphism ("Tauernkristallisation" of SANDER, 1921), especially in the Upper Schieferhülle, are known from e.g. the studies of HOERNES and FRIEDRICHSEN (1974), RAASE and MORTEANI (1976), HÖCK (1980), HÖCK and HOSCHEK (1980), OXBURGH and TURCOTTE (1974), OXBURGH and ENGLAND (1980), SATIR and FRIEDRICHSEN (1986), SELVERSTONE et al. (1984), SELVERSTONE and SPEAR (1985), DROOP (1985) and BLANCKENBURG et al. (1989). Compared to the large amount of work

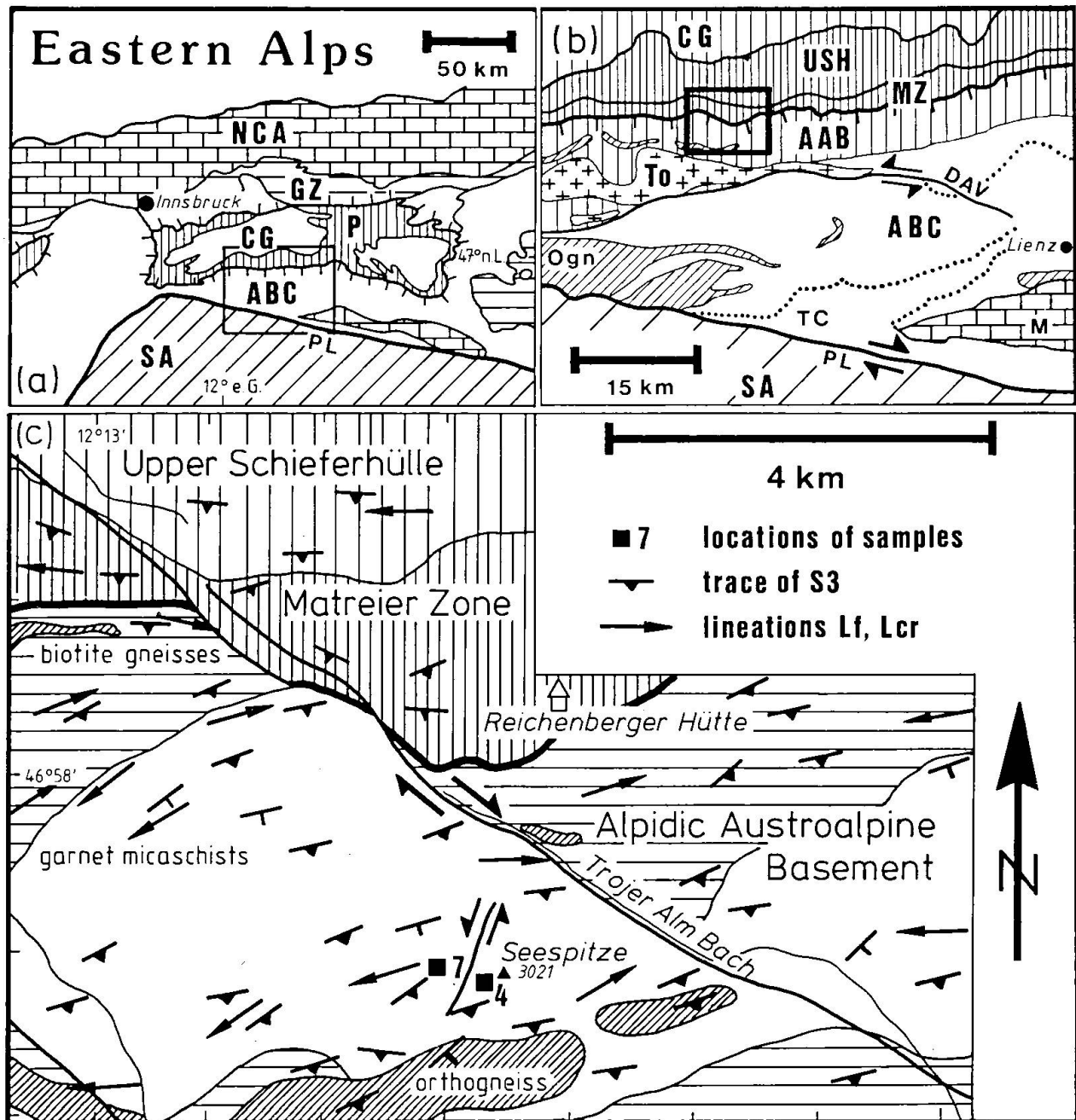


Fig. 1 Geological setting (a), (b) and structural geology (c) of the sampled area. Lithology and structures after SENARCLENS-GRANCY (1972) and ZARSKÉ (1985). AAB – Alpidic Austroalpine basement; ABC – Austroalpine basement complex; CG – Central gneisses of Tauern Window; DAV – Deferegggen-Antholz-Vals-Line; M – Permomesozoic of Drau; MZ – Matreier Zone; PL – Periadriatic Lineament; TC – Thurmtaler complex; To – tonalite; SA – Southern Alps; USH – Upper Schieferhülle.

which has been done in the Tauern Window (for further bibliography see FRANK et al., 1987 and FRISCH et al., 1987), only a few new petrologic data exist for the Alpidic part of the Austroalpine basement to the south of the Tauern Window (e.g. CONTINI and SASSI, 1980; HOFMANN et al., 1983; STÖCKHERT, 1984, 1985).

This paper deals with the determination and tectonic interpretation of a P-T-t-deformation path from Alpidic Austroalpine garnet-micaschists three kilometers above the Matreier Zone and the Upper Schieferhülle. The obtained prograde-retrograde path is not smoothly curved. Its edges give crucial hints at the early-Alpine tectonic and metamorphic evolution during a continental collision.

## 2. Structures

Several samples from garnet-micaschists were collected in the Seespitze area, northern Deferegggen Alps, Tyrol, Austria (Fig. 1c). These garnet-micaschists, called Cima-Dura-phyllites elsewhere (DAL PIAZ, 1934; BAGGIO et al., 1971), are very uniform in their mineralogic composition and accompany the southern frame of the Tauern Window. The rocks in the sampling area are uniform as well and all samples have quite similar compositions with muscovite 35%, quartz 25%, biotite 16%, garnet 7%, plagioclase 7%, chlorite 6%, ilmenite 3%, epidote 1% (sample 7, 500 points counted). Biotite gneisses with intercalated orthogneisses are found to the south and separate the garnet-micaschists from the Matreier Zone to the north. Although belonging to the pre-Alpine Austroalpine basement, the garnet-micaschists are considered to be completely overprinted by Alpine events, as is obvious from radiometric and structural data (BORSI et al., 1978; STÖCKHERT, 1984, 1985).

A weakly crenulated main foliation S3 (see below) strikes ENE-WSW and dips steeply to the south (S 74 / 78 S). Lineations by open crenulation Lcr4 and fold axes Lf plunge gently to ENE or WSW (L 70 / 10 W) (Figs 1c, 2). Most obvious mesoscopic structures are isoclinal folds (F3) of quartz layers and quartz rods which are elongated some meters parallel to L. A shearband foliation S4 crosscuts S3 at high angles (Fig. 2a). Similar structures are found in the underlying Matreier Zone and the Upper Schieferhülle which are positioned about 3 km below the sampled area. Such structurally concordant transitions from the Austroalpine basement into the underlying Mesozoic units were also macroscopically and mesoscopically observed by NOLLAU (1969) to the west and by BARNICK (1965) and BEHRMANN and WALLIS (1987) to the east.

## 3. Microstructures

About 40 thin sections in XZ- and YZ-planes, defined by the main lineation L (see Fig. 2) were studied from seven samples which all show similar meso- and microstructures. Foliation S3, composed of planar biotite, muscovite and chlorite (Bt2, Ms2, Chl) is the most significant structure in the sections (Fig. 2b). The S3 foliation surrounds quartz-rich microlithons which contain abundant quartz, rare epidote and a relic crenulation foliation S2 underlined by biotite 1 and muscovite 1. Structurally zoned garnets (Grt) inside the microlithons have S-shaped inclusion trails of S1-Si, defined by quartz, epidote and heavy minerals, in their cores. Biotite (Bt3) and chlorite are sometimes found in pressure-shadow positions close to the porphyroblasts. Optically weakly zoned plagioclases (An 2-3 determined by microprobe) mostly occur in S3 planes and enclose opaque minerals (Fig. 4e). The plagioclase porphyroblasts with irregular grain boundaries seem to have grown at the expense of muscovite. Other plagioclases with similar compositions and similar shapes are found inside the microlithons. These porphyroblasts are probably completely converted older plagioclases formerly richer in anorthite. Foliation S3, crossed by large biotites, muscovites and chlorites (Bt3, Ms3), was slightly deformed by a late foliation S4 underlined by chlorite (Fig. 2b).

S1-Si inclusion trails are planar or smoothly curved in the innermost part of the garnets. This indicates a static growth of the porphyroblasts. To an intermediate zone, sometimes openly and tightly curved hinges of S1-Si at each side of the porphyroblasts are observed (Fig. 4a). Broad rims without any inclusions point to a final static growth synchronous to the formation of S2.

The significance of S-shaped inclusion trails inside porphyroblasts is still controversial: BELL (1985) and BELL and JOHNSON (1989) found evidence of a static growth and no syncrystalline rotation of such porphyroblasts during deformation histories of progressive bulk shortening. In contrast, SCHONEVELD (1977) and MASUDA and MOCHIZUKI (1989) modelled a syncrystalline rotation of circularly growing porphyroblasts by shearing. However, the differently curved hinges of inclusion trails at each side of the garnets are very similar to the inclusion trails shown by SCHONEVELD (1977) and MASUDA and MOCHIZUKI (1989). A circular (spherical) growth of the garnets is proved by chemical profiles (Figs 4a, 4b). For this reason the observed S-shaped inclusion trails probably indicate a short period of syncrystalline porphyroblast rotation.

Sample 4 was studied intensely to obtain more information about shear senses and deformation

history. All 23 garnets with inclusion trails out of 46 porphyroblasts in a XZ-section (Fig. 2b) show clockwise rotation around Y (POWELL and TREA-

GUS, 1969). In the YZ-section, out of 50 garnets only 10 examples with curved inclusion trails show clockwise rotation and 17 porphyroblasts contain

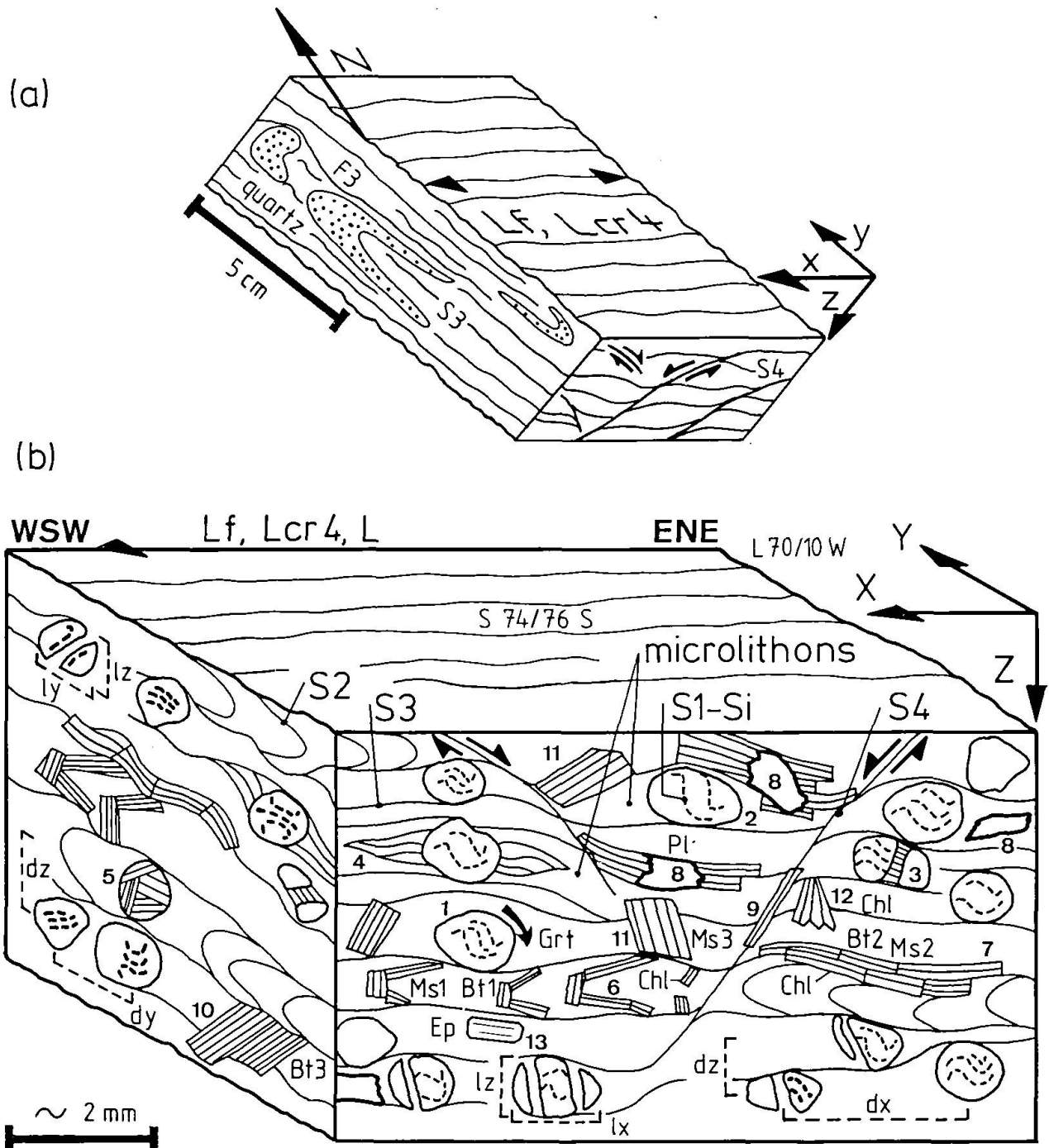


Fig. 2 (a) Mesoscopic structures of garnet-micaschists.

(b) Microstructural relationships inside garnet micaschists in a synoptic view, compiled from samples 4 and 7.

1 – garnet (Grt) with S-shaped inclusion trails of S1-Si which indicate syncrystalline rotation around Y-axis (see Fig. 4a), rotation sense may be inverted by isoclinal folding F3 around Lf. 2 – garnet with oriented dissolution at contact to S3 plane; 3 – garnet with tension cracks filled by chlorite (Chl); 4 – garnet with pressure-shadows of biotite (Bt3); 5 – chlorite pseudomorph is replacing garnet; 6 – biotite, muscovite (Bt1, Ms1), chlorite, forming crenulated foliation S2 (see Fig. 4d); 7 – biotite, muscovite and chlorite (Bt2, Ms2, Chl) forming crenulation foliation S3; 8 – plagioclases An 2-3 (Pl) in S3 foliation plane (see Fig. 4e) and inside microlithon. The plagioclase inside the microlithons seems to be converted older plagioclase. 9 – chlorite in S4 shear plane; 10, 11, 12 – muscovite, biotite and chlorite (Ms3, Bt3, Chl) cutting foliation S3; 13 – idiomorphic epidote (Ep) inside microlithon. dx, dy, dz – spacing between garnets of one cluster; lx, ly, lz – dimensions of garnets with tension cracks. X, Y, Z – reference axes.

planar inclusion trails. Similar relationships were found in two further samples; oppositely directed rotation senses around Y were observed in two other samples. Such incoherent garnet rotation senses from different samples probably were caused by isoclinal folding F3 around Lf (Fig. 2a).

The S1-Si inclusion trails inside the garnets do not line up with the crenulated foliation S2. An oblique orientation of S2 with an unknown, but constant angle in reference to the XY-plane previous to D3 may be inferred from the relatively constant positions of the inclusion trails within the XYZ-frame (Fig. 2b). Thus, from these geometric relationships, only a shearing in the S2-plane perpendicular to the Y-axis can be derived. A regional sense of shear or transport is not available from the existing data.

A clustered arrangement of the garnets in the sample (Fig. 2b) allows no simple application of center-to-center methods (RAMSEY and HUBER, 1983) to determine bulk strain. This arrangement is a consequence of the crenulation folding of S2 and was not caused by a clustered garnet growth previous to formation of S2. However, the distances in the XY- and Z-directions between the garnets of a cluster are significantly different. Six dx/dz ratios (Fig. 2b) from 3.0 to 5.1 and seven dy/dz ratios from 1.1 to 6.5 in sample 4 may indicate a flattening in the XY-plane.

As is obvious from the chemical profiles, the garnets in the samples were initially circular (spherical), but some porphyroblasts are corroded at the contacts with the surrounding foliation S3. Tension cracks of other garnets are filled by chlorite (Fig. 2b). Out of 48 garnets in the XZ-section of sample 4, 20 examples show tension cracks. The lx/lz ratios (Fig. 2b) vary at about 1.67. Only 4 garnets out of 50 porphyroblasts in the YZ-section display tension cracks and have a ly/lz ratio of 1.35. These relationships indicate an axial extension (constriction) in X-direction. The slight coherent obliquity of the tension cracks in reference to the Z-direction (Fig. 2b) may give a hint of a contemporaneous small simple shear deformation component.

A deformation history was deduced semiquantitatively from these observed microstructural relationships. Temporally changing amounts of simple shear and pure shear deformation components produced a finite state of deformation. Foliations S1 and S2 were generated during a deformation sequence D1-D2. It is difficult to evaluate the type of dominant deformation and the primal orientation of S2-planes related to this sequence. However, rotated garnets recorded a period of an increased simple shear deformation component with a shearing direction perpendicular to Y and a considerable simple shear component can be assumed in course

of the generation of S2. Subsequently, deformation D3 crenulated the S2 foliation. This deformation sequence was dominated by pure shear deformation components (flattening/constriction, see above) as is indicated by the strain data and the undisturbed angular relationships between the garnet rotation axes and the X-axis. Nevertheless, an additional minor simple shear deformation component led to the crenulation foliation S3. The presently observed orientation of S3 (Fig. 1b) was caused by later large-scale updoming/shortening of the Tauern Window and its frame (LAMMERER, 1988).

#### 4. Mineral assemblages

A mineralogical-microstructural scheme (Fig. 3), which shows the successive appearance of mineral phases in the course of time, was recognized from the microstructural relationships in samples 4 and 7. These samples contain the same phases in similar microstructural positions and are considered to represent the typical microstructural evolution of the garnet micaschists. The successive appearance/disappearance of mineral assemblages can be seen in this scheme.

An early assemblage M1: garnet, biotite 1, muscovite 1, chlorite, plagioclase (disappeared), quartz and epidote represents an upper greenschist facies metamorphism during the D1-D2 deformation sequence. A later assemblage M2: biotite 2, muscovite 2, chlorite, plagioclase, quartz and epidote probably characterizes a change to lower temperatures in the course of D3.

#### 5. Mineral compositions

About 60 chemical analyses of mineral grains were obtained by microprobe in an XZ-section of sample 7 and are summarized in Tab. 1. Garnets are strongly zoned: Spessartine (Sps) and grossular (Grs) contents discontinuously decrease from cores to rims, Mg/Mg + Fe<sup>2+</sup> contents are constant up to the intermediate zones and then increase continuously to the outer rims (Fig. 4b). The general trend of this chemical evolution (Fig. 4c) qualitatively signals increasing temperatures and decreasing pressures (MARTIGNOLE and NANTEL, 1982). A significant constant or slightly increasing grossular component in the intermediate zones and then steeply falling grossular contents in the rims interrupt this general tendency (Figs 4b, 4c). These chemical variations were observed from several porphyroblasts in the section.

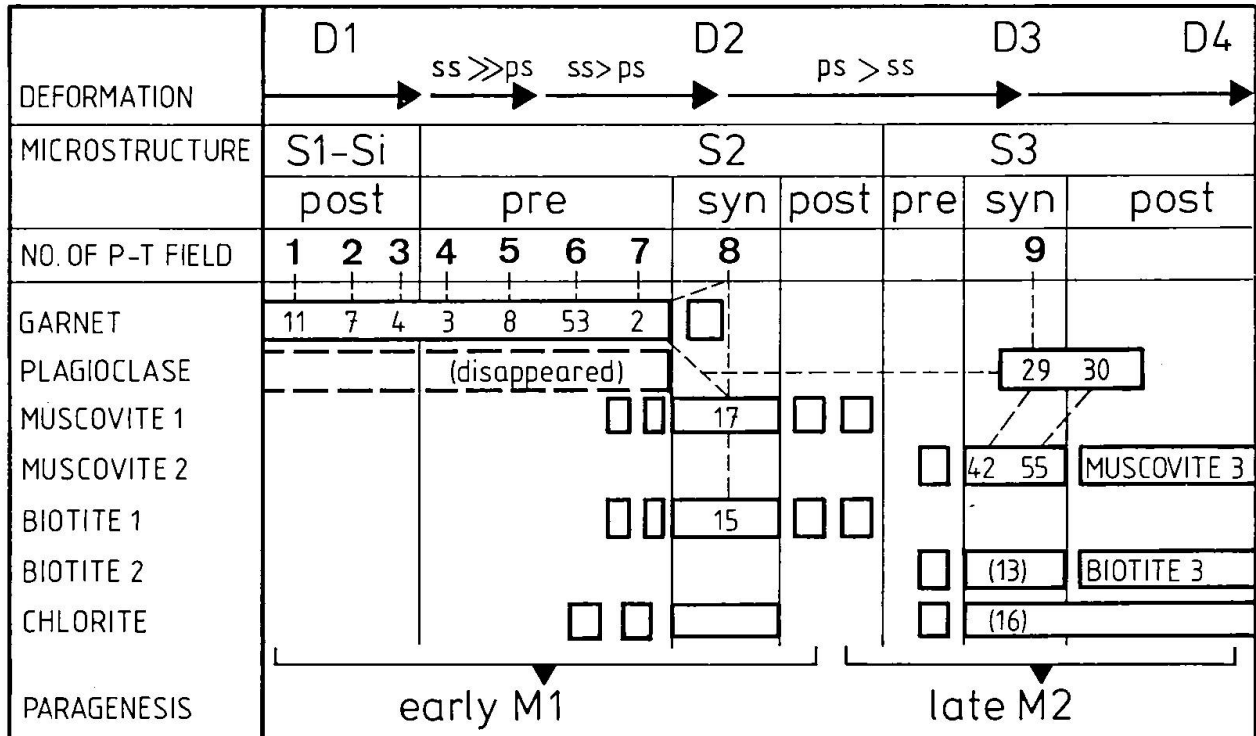


Fig. 3 Appearance of minerals in course of time, derived from their structural positions relative to foliations S1 to S3, compiled from samples 4 and 7. Numbers identify microprobe analyses in Tab. 1, bold numbers indicate calculated P-T fields in their positions relative to microstructures, broken lines connect the analyses which were combined to calculate relative P-T variations (see Fig. 5a). D1 to D4 – phases of deformation; ss – simple shear deformation component with shearing perpendicular to Y; ps – pure shear deformation component; M1, M2 – successive mineral assemblages; disappeared plagioclase in assemblage M1 probably was completely converted to the younger plagioclase.

The three generations of biotite are quite similar in their chemical composition: biotites 1 in S2-position vary in XMg from 0.44 to 0.46; biotites 2 in foliation S3 have a XMg of 0.44. Third generation biotites show slightly lower values of XMg from 0.44 to 0.42. Similarly, S2-biotites are slightly richer in Ti (0.22) than biotites from S3 (Ti = 0.19 p.f.u.).

Significantly different chemical compositions were observed in syn-S2 and syn-S3 muscovites. S2-muscovites (Ms1) are richer in Na and poorer in Si<sup>4+</sup>, Mg, Fe than S3-muscovites (Ms2) (Figs 4f, 4g). From these chemical differences it can be concluded that S2 was generated at higher temperatures than S3 and that pressures only slightly changed from S2 to S3 (CIPRIANI et al., 1971).

## 6. Estimations of P-T variations

The constant or slightly increasing grossular contents in the intermediate zones of the garnets are closely related to the curvature of the S-shaped inclusion trails (Figs 4 a, b, c) which indicate a significant deformational event within the deformation sequence D1-D2. In the same way, the signifi-

cant change in mineral chemistry of the muscovites in foliations S2 and S3 corresponds to the deformation D3. These small-scale deformations of the rocks were induced by large-scale tectonic events which influence the evolution of P and T in the crust. In consequence, the observed chemical variations, closely related to deformations, may correspond to variations of P and T. In particular, garnet compositions can continuously change by continuous reactions and reflect temporal changes of P and T (TRZCIENSKI, 1977; TRACY, 1982). On the other hand, micas in successive foliations represent discontinuous steps of the P-T evolution (TRIBOULET and AUDREN, 1985).

The phyllosilicates continuously recrystallize in the foliation planes during progressing deformation. Thus, their chemical compositions are related only to the final increment of each deformation phase and represent discontinuous chemical markers in a scenario of successive deformations. This explains the quite homogeneous compositions of micas in each foliation generation.

The calculation of several successive values of P and T from metapelitic mineral assemblages requires chemical data from garnets, biotites, musco-

Tab. 1 Selected microprobe analyses of garnets (24 O), biotites (22 O), muscovites (22 O), chlorite (28 O) and plagioclases (8 O). For microstructural positions of the analyses see Figs 3, 4. Foliation S2 is formed by biotite 1 and muscovite 1; foliation S3 is formed by biotite 2 and muscovite 2. All analyses are from sample 7.

	core		garnet					rim	plagioclase	
	11	7	4	3	8	53	2	29	30	
SiO <sub>2</sub>	36.43	36.37	36.38	36.60	36.79	36.48	36.10	SiO <sub>2</sub>	70.27	69.35
TiO <sub>2</sub>	.18	.04	.09	.12	.00	.03	.03	CaO	.44	.58
Al <sub>2</sub> O <sub>3</sub>	20.35	20.34	20.59	20.71	20.39	20.67	20.95	Na <sub>2</sub> O	10.51	10.01
FeO	29.88	34.80	35.59	36.36	36.70	38.38	38.75	K <sub>2</sub> O	.04	.07
MnO	7.06	3.01	2.68	1.70	.98	.95	.57	Al <sub>2</sub> O <sub>3</sub>	20.72	20.33
MgO	.95	1.50	1.59	1.81	2.31	2.36	2.67	tot	101.98	100.34
CaO	3.97	2.87	2.20	2.06	1.89	.79	.33	Si	2.99	2.99
tot	98.82	98.93	99.12	99.36	100.06	99.83	99.40	Ca	.02	.02
Si	5.98	5.98	5.97	5.90	6.02	5.95	5.98	Na	.86	.83
Al	3.94	3.94	3.98	3.98	3.93	3.98	4.04	K	.00	.00
Fe <sup>2+</sup>	4.10	4.78	4.88	4.97	5.02	5.24	5.30	Al	1.03	1.03
Mn	.98	.42	.37	.23	.13	.13	.07	tot	4.90	4.87
Mg	.23	.37	.38	.44	.56	.57	.65	An	2.23	3.07
Ca	.69	.50	.38	.36	.33	.13	.05			
tot	15.92	15.99	15.96	15.88	15.99	16.00	16.09			
Alm	68.36	78.76	81.06	87.09	82.99	86.14	87.09			
Sps	16.36	6.91	6.18	3.92	2.25	2.17	1.29			
Prp	3.87	6.07	6.44	7.36	9.29	9.46	10.71			
Grs	10.94	8.04	6.09	5.58	5.43	2.12	.83			
	_____ S2 _____		muscovite _____ S3 _____			_____ S2 _____ biotite _____ S3 _____			chlorite	
	17	18	42	55	26	15	13	21	16	
SiO <sub>2</sub>	51.02	50.90	52.20	53.00	53.13	37.10	36.53	36.25	24.40	
TiO <sub>2</sub>	.40	.30	.30	.30	.30	1.95	1.72	1.72	.00	
Al <sub>2</sub> O <sub>3</sub>	36.03	34.93	32.16	32.19	31.92	17.84	18.00	18.28	22.06	
FeO	1.52	1.54	2.28	2.32	2.31	20.15	20.13	20.21	26.03	
MgO	1.18	1.20	2.21	2.32	2.24	9.05	9.01	9.08	13.73	
Na <sub>2</sub> O	1.01	.97	.67	.47	.56	.22	.24	.24	.01	
K <sub>2</sub> O	7.25	7.78	7.28	6.32	7.63	8.03	8.23	8.02	.00	
tot	98.41	97.62	97.10	96.92	98.09	94.34	93.86	93.80	86.23	
Si	6.41	6.47	6.66	6.72	6.71	5.62	5.60	5.56	5.24	
Ti	.03	.03	.03	.03	.03	.22	.19	.19	.01	
Al	5.33	5.23	4.84	4.81	4.75	3.20	3.25	3.30	5.59	
Fe <sup>2+</sup>	.15	.16	.24	.24	.24	2.56	2.58	2.59	4.68	
Mg	.22	.22	.42	.43	.42	2.05	2.06	2.07	4.40	
Na	.24	.23	.16	.11	.13	.06	.07	.07	.00	
K	1.16	1.26	1.18	1.02	1.23	1.56	1.61	1.57	.00	
tot	13.54	13.60	13.53	13.58	13.51	15.27	15.36	15.35	19.92	

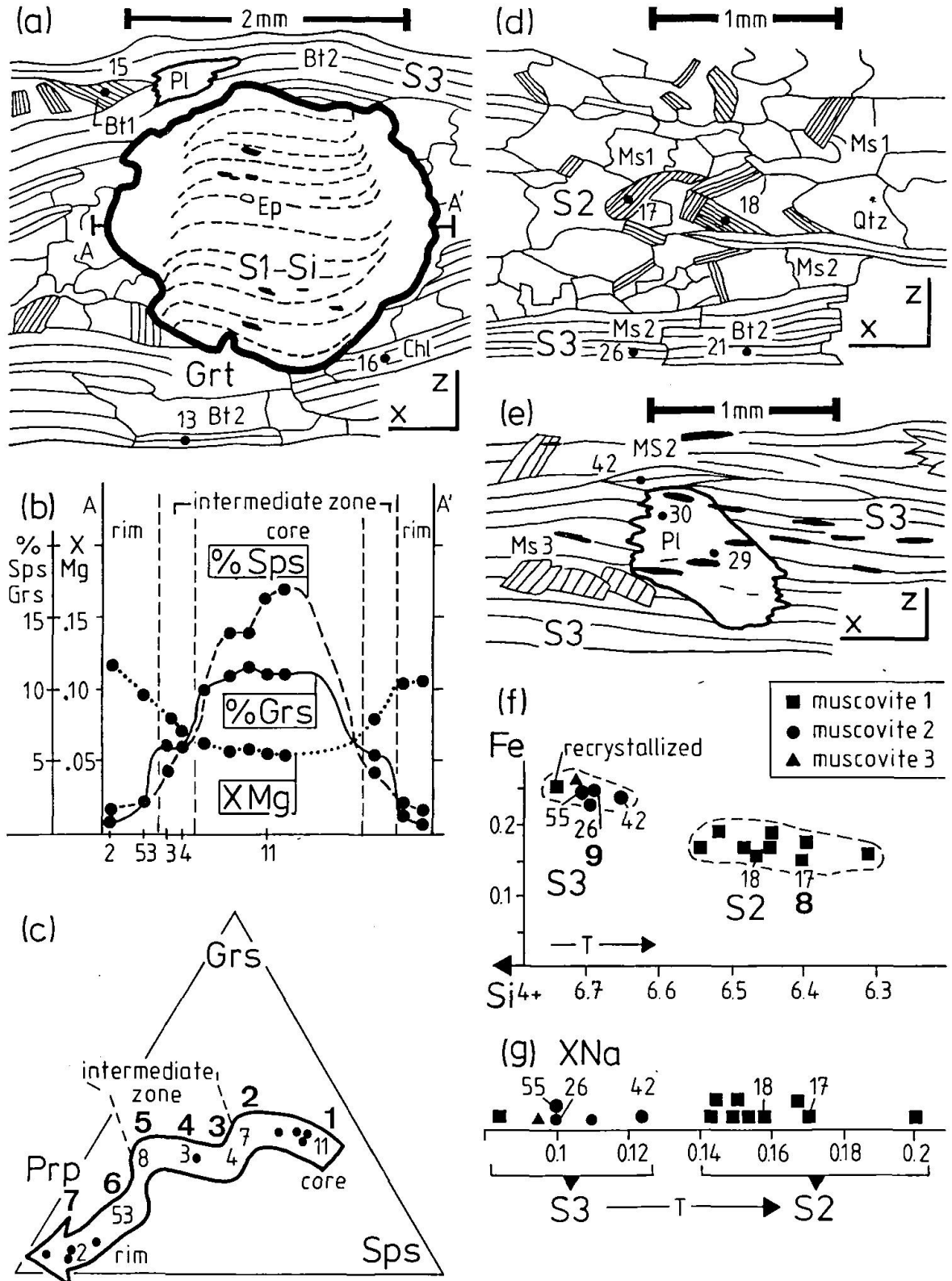


Fig. 4 (a) Garnet (Grt) with sharply and openly curved S1-Si inclusion trails at each side. The porphyroblast is situated in a microlithon wrapped by S3. Numbers identify microprobe analyses from adjacent minerals. (b) Chemical profile of the garnet in Fig. 4a with spessartine (Sps), grossularite (Grs) and Mg/Mg + Fe<sup>2+</sup> contents. (c) Evolution of garnet compositions in grossularite (Grs) - spessartine (Sps) - pyrope (Prp) coordinates; numbers identify analyses of Tab. 1, bold numbers indicate calculated P-T fields. (d) Crenulated foliation S2 in microlithon which is surrounded by crenulation foliation S3. Numbers identify microprobe analyses in Tab. 1. (e) Plagioclase (Pl) in S3 foliation plane. (f) Chemical properties of white micas from foliations S2 (muscovite 1) and S3 (muscovite 2) in Fe-Si coordinates. Numbers show analyses of Tab. 1, bold numbers identify calculated P-T fields. (g) Na contents of white micas in foliations S2 and S3.

vites and plagioclases coexisting during corresponding time intervals  $\Delta t$ . As is obvious from the mineralogical-microstructural scheme (Fig. 3), due to the very different times of appearances, the late plagioclase is not compatible with garnet. Early oligoclase and andesine coexisting with garnet are known (ZARSKE, 1985) from biotite gneisses and garnet-micaschists in the region. In the analyzed samples such plagioclase was not found and the sole observed Ca-bearing mineral found coexistent with garnet is accessoric epidote.

However, the garnet must have exchanged Ca with a coexisting abundant solid or liquid medium in close dependence on the deformation as is obvious from its discontinuous chemical zonations. A complete conversion of pre-existing plagioclase richer in anorthite to the observed younger plagioclase by further reactions (probably  $Ms1 + Pl1 + H_2O = Ms2 + Pl2$ ) in course of the metamorphism seems to be a satisfying explanation. This is supported by the observation of late plagioclase inside microlithons nearby garnet (Fig. 2b). Replacement of early plagioclase by epidote induced by exaggerated fluid migration from underlying mesozoic metasediments (STÖCKHERT, 1982) may be also taken into account.

Due to the lacking analyses from the disappeared early plagioclase, no absolute, but only relative pressure variations may be calculated from the garnet zonations. Furthermore, the micas from foliation S2 grew contemporaneously with the garnet rims and there are some time intervals  $\Delta t$  of coexistence during late stages of garnet growth. This allows calculation of the variations in T in relation to the temperature reached during the final stage of garnet growth.

Methods proposed by SPEAR and SELVERSTONE (1983) to estimate P and T from garnet zoning cannot be applied directly due to the incomplete existing pre/syn-S2 mineral assemblage (M1) in the sampled garnet-micaschists. A different method, based as well on the garnet zoning, was used. Input of always the same biotite, muscovite and inadequate plagioclase compositions into the calculations gives a systematic error in the results. However, this systematic error does not affect the principal sense of the calculated P-T variation (SPEAR and RUMBLE, 1986).

Relative temperatures and pressures were calculated by combining several garnet analyses with always the same syn-S2 biotite and muscovite and an inadequate plagioclase, treating biotite, muscovite and plagioclase as a constant factor (Fig. 3). Thus, the obtained P-T variation is only dependent on garnet compositions and reflects a relative P-T variation directly dependent on the discontinuous zonation.

The data from garnet and biotite was applied using seven pressure-dependent geothermometric calibrations. Only maximal and minimal results from calibrations by THOMPSON (1976), HOLDAWAY and LEE (1977), HODGES and SPEAR (1982) and PERCHUK and ARANOVITCH (1984) are shown (Fig. 5a). The variations in temperatures from 500 °C (garnet core and S2-muscovite) to 580 °C (garnet rim and S2-muscovite), calculated by the geothermometer of GREEN and HELLMANN (1982) is not as broad than from the garnet-biotite calibrations. However, syn-S2 temperatures are similar from all applied geothermometers.

The relative variations in pressure by calculations with the calibration of GHENT and STOUT (1980), involving garnet, biotite, muscovite and the inadequate late plagioclase is shown by Fig. 5a. The pressure-dependent transission of  $Al^{VI}$  to  $Al^{IV}$  and of  $Mg, Fe^{VIII}$  to  $Mg, Fe^{VI}$  in micas involved in the calibration was kept constant by the procedure described above and only net transfer of Ca between garnet and the intentionally used inadequate plagioclase is taken into account for relative pressure determination. Thus, the results depend strongly on the garnet activity model of GHENT and STOUT (1980), which is calibrated for rocks with lacking aluminosilicates. Other calibrations from GHENT (1976) and NEWTON and HASELTON (1981), applied to draw error surfaces, produced pressure values systematically higher and with a similar sense of variation. Calculations with an assumed oligoclase led to the same sense of variation.

However, all these calibrations involve the garnet activity model as a predominant part, and micas and plagioclase as minor parts of the calculations. Thus, the results will always depend strongly on the chemical zonation of the garnet, even if chemical compositions of inadequate associated minerals are intentionally integrated. As was pointed out by SPEAR and RUMBLE (1986), such an (intentional) input of a systematic error like the chemical composition of an inadequate plagioclase into the calculations will not reverse the sense of the P-T variation and therefore will not affect the principal shape of the relative P-T path.

For the above mentioned reasons, the calculated values of pressures in the P-T fields 1 to 7 are not realistic and too high and reflect only a relative change of metamorphic conditions in an interval of 4.5 kbar. Values of temperatures are realistic, especially the maximum temperature which was calculated from minerals in adjacent positions on the microstructural-mineralogical scheme (Fig. 3).

It is possible to estimate minimum pressures from  $Si^{4+}$  contents of white micas coexisting with biotite and quartz (VELDE, 1967; MASSONNE and SCHREYER, 1987) if temperatures are known. The

Si<sup>4+</sup> contents of representative muscovites from foliations S2 and S3 (Figs 4 f, g) previously were normalized by subtracting the paragonite component and recalculating the structural formulae (DJRO et al., 1989).

As is obvious from high pyrope components (Fig. 4c) and the microstructural observations (Fig. 3), the rims of the garnets grew at maximum temperature contemporaneous with the formation of foliation S2. This is also proved by qualitative geothermometry (CIPRIANI et al., 1971) from S2-muscovites which indicates a growth of these micas at high temperatures (Figs 4 g, f). Accordingly, lower temperatures can be assumed during the formation of S3. Two extreme compositions of S3-muscovites combined with analyses of plagioclases which grew also in S3 were calculated by the geothermometer of GREEN and USDANSKY (1986). Then the similar results from garnet-biotite- and garnet-phengite-thermometry (Fig. 5a, P-T field 7) fixing the temperature of S2-formation ( $\triangleq T_{\max}$ ), and results from plagioclase-phengite-thermometry which fix the temperature of S3-formation were combined with the minimum pressures from Si<sup>4+</sup> contents of S2- and S3-muscovites (VELDE, 1967). This led to the P-T fields 8 and 9 (Fig. 5a).

Next the pre/syn-S2 P-T path from the garnets was connected with the syn/post S2 path from the muscovites. The combined path displays the relative P-T evolution prior and subsequent to the for-

mation of S2 which is fixed at a well-defined  $T_{\max}$  and a corresponding minimum pressure (Fig. 5b). In spite of the relativity of this P-T evolution in relation to the P-T conditions syn-S2, all actual P and T of the assembled path (Fig. 5b) are consistent with data from other authors (STÖCKHERT, 1984; SELVERSTONE and SPEAR, 1985; DROOP, 1985). Thus, this path seems to represent a reliable result. Whatever the actual values of this assembled path are, the shape of this P-T path is significant for its thermotectonic interpretation. The principal shape is only dependent on the chemical evolution of the garnets and the micas and will not be affected by inaccurate thermodynamic data, inaccurate geothermobarometry, or input of compositions of inadequate associated minerals (SPEAR and RUMBLE, 1986). Consequently, the close relationships between rock deformation and chemical variations / P-T variations can be used to evaluate a large-scale tectonic scenario from the shape of this P-T-deformation path.

### 7. Tectonic significance of the P-T path

Numerical modelling of crustal evolutions is a basis for the tectonic interpretation of P-T paths from metamorphic rocks. The clockwise sense of the obtained path is characteristic of tectonic thickening and subsequent uplift of continental crust (ENG-

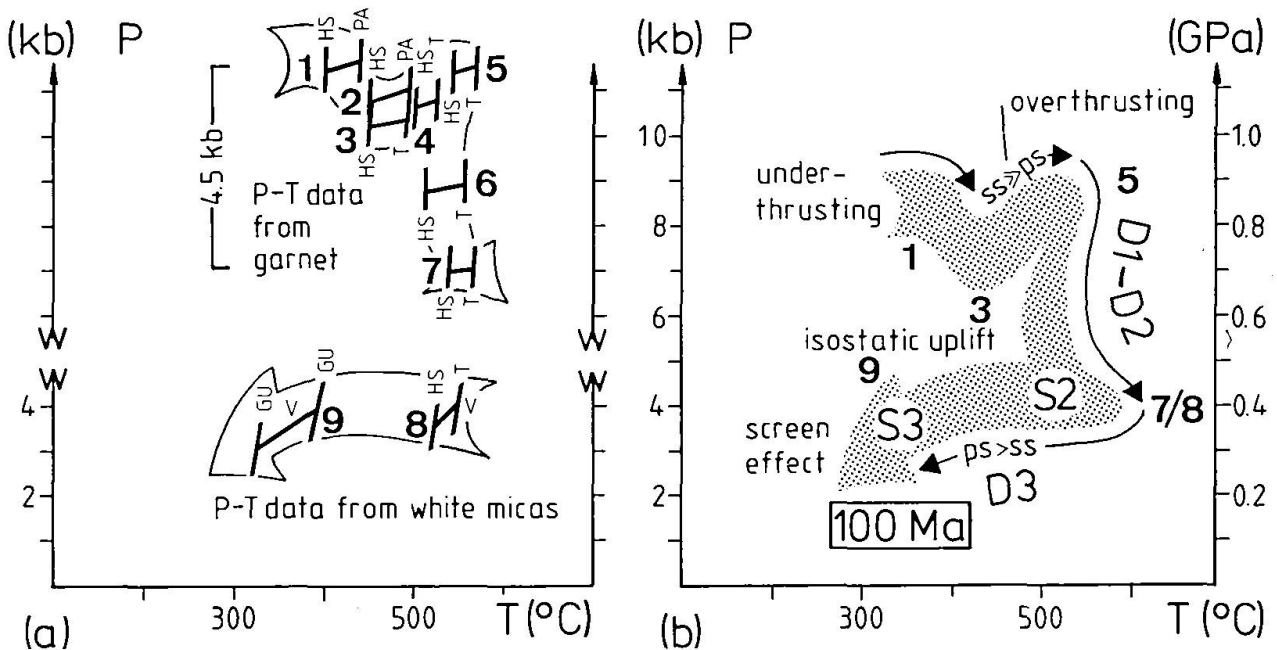


Fig. 5 (a) Estimated P-T paths; P-T fields which define global error of calculations are marked by bold numbers, microstructural positions of P-T fields see Fig. 3. Abbreviations of geothermometers: GU – GREEN and USDANSKY (1986); HS – HODGES and SPEAR (1982); PA – PERCHUK and ARANOVITCH (1984); T – THOMPSON (1976). Calibrations from VELDE (1967) (V) and GHENT and STOUT (1980) were used for geobarometry. (b) P-T-t-deformation path from garnet-micaschists of the Alpidic Austroalpine basement, compiled from the paths in Fig. 5a. The shape of the path characterizes several tectonic events. See text and Fig. 6 for further explanations.

LAND and THOMPSON, 1984; THOMPSON and ENGLAND, 1984; SPEAR et al., 1984). Stacking by under- and overthrusting of several tectonic units is considered to be an important process of such thickening of crust. Modelled underthrusting of a first tectonic slab beneath a pre-existent crust and the succeeding isostatic uplift of this slab (DAVY and GILLET, 1986) resulted in post- $P_{\max}$  paths similar to the general shape of the observed prograde T-retrograde P evolution of the garnet-micaschists. A modelled further understacking of a second tectonic unit beneath the first unit then led to an isobaric temperature-decrease in the first slab. This is caused by a covering effect of the initially cold second unit (DAVY and GILLET, 1986; AUDREN and TRIBOULET, 1988). Such an isobaric temperature-decrease ("screen effect") is observed as well in the garnet-micaschists (Fig. 5b).

The re-increasing pressures at increasing temperatures in the first segment of the path can be explained by an overthrusting of a tectonic slab (DAVY and GILLET, 1986; SPEAR and RUMBLE, 1986). Similar shapes of early post- $P_{\max}$  paths were observed in the western and eastern parts of the Upper Schieferhülle and the allochthonous Lower Schieferhülle by SELVERSTONE and SPEAR (1985), SELVERSTONE et al. (1984) and DROOP (1985). This implies coherent Alpine P-T histories in the Alpidic Austroalpine basement and the underlying units listed above.

Therefore the thermotectonic evolution of the Alpidic Austroalpine basement may tentatively be modelled by combining the Upper Schieferhülle / allochthonous Lower Schieferhülle, the Matreier Zone and the Austroalpine basement into one tectonic unit. This combination of the subunits is based mainly on the similar shapes of the early post- $P_{\max}$  paths and the parallel structures in the lithological units. Further detailed research probably will lead to other combinations of subunits. A schematic palaeogeographic arrangement of the lithologic units previous to a collision is shown in Fig. 6a. The three united lithologic units, forming a tectonic unit 1 (Fig. 6b) were underthrust to the south beneath the Austroalpine basement and suffered a common high pressure - low temperature (HP-LT) metamorphism at 8 kbar / 400 °C (Figs 5b, 6c). The subsequent isostatic uplift of the thickened crust was interrupted by the overthrusting of a tectonic slab with a minimum thickness of 3 km. This overthrusting event coincides with the syn-crystalline garnet rotation (Fig. 6d). On account of the palaeogeographic situation, this overthrust slab must come from the south or southeast and may be the Upper Austroalpine Unit.

A sharp pressure-decrease and a minor decrease in temperature were caused by an exag-

gerated isostatic uplift and shortly sinking isotherms after overthrusting (Fig. 6d). Temperatures then slightly increased up to  $T_{\max}$  of 550 °C and pressures further decreased down to 4 kbar. A subsequent significant isobaric temperature decrease to 3.5 kb / 350 °C is the result of an understacking of cold European crust (Central gneisses / autochthonous Lower Schieferhülle, tectonic unit 2) under unit 1 (Fig. 6e). As it was modelled by DAVY and GILLET (1986), the screen effect played by this tectonic unit 2, will be efficient for time delays between the two underthrusting events of less than 30 million years. It is important to note that in unit 1, now acting as a hangingwall, a significant change from non-coaxial deformation to predominant pure shear deformation during the understacking of unit 2 is observed. The temporally changing type of deformation seems to be directly related to the position of the tectonic units within the collision scenario (ELLIS and WATKINSON, 1987).

K-Ar isochrons of about 100 Ma from small recrystallized white micas in the main foliation of pegmatites which were affected by Alpine deformation (STÖCKHERT, 1984) give the ages of cooling below  $350 \pm 50$  °C (JÄGER, 1979). The relative position of this age determination on the P-T path coincides approximately with the formation of S3 at the end of the recorded P-T evolution. This suggests an early Cretaceous age of the underthrusting and overthrusting events. Rb-Sr isochrons from biotites in the Alpidic Austroalpine basement and the adjacent southern part of the Tauern Window vary between 28 and 16 Ma (BORSI et al., 1978). These ages are continuously younger from south to north and indicate different rates of late-Alpine uplift and cooling below  $300 \pm 50$  °C (JÄGER, 1979) in the Tauern Window and its southern frame (GRUNDMANN and MORTEANI, 1985). The data implies a long period of very slow uplift/cooling rates in the Alpidic Austroalpine basement between 100 and 30 Ma (STÖCKHERT, 1984). This induced static annealing of fabrics (STÖCKHERT, 1982; KLEIN-SCHRODT, 1987).

## 8. Conclusions

A close relationship between deformation history and evolution of mineral chemistry was used to construct a combined P-T-deformation path, assembled by relative P-T variations from garnet zoning and from muscovites in successive foliations.

The shape of the obtained P-T-t-deformation path provides detailed information about the temporal, spatial and thermotectonic evolution of the Alpidic Austroalpine basement during the early-Alpine continental collision. Understacking of the

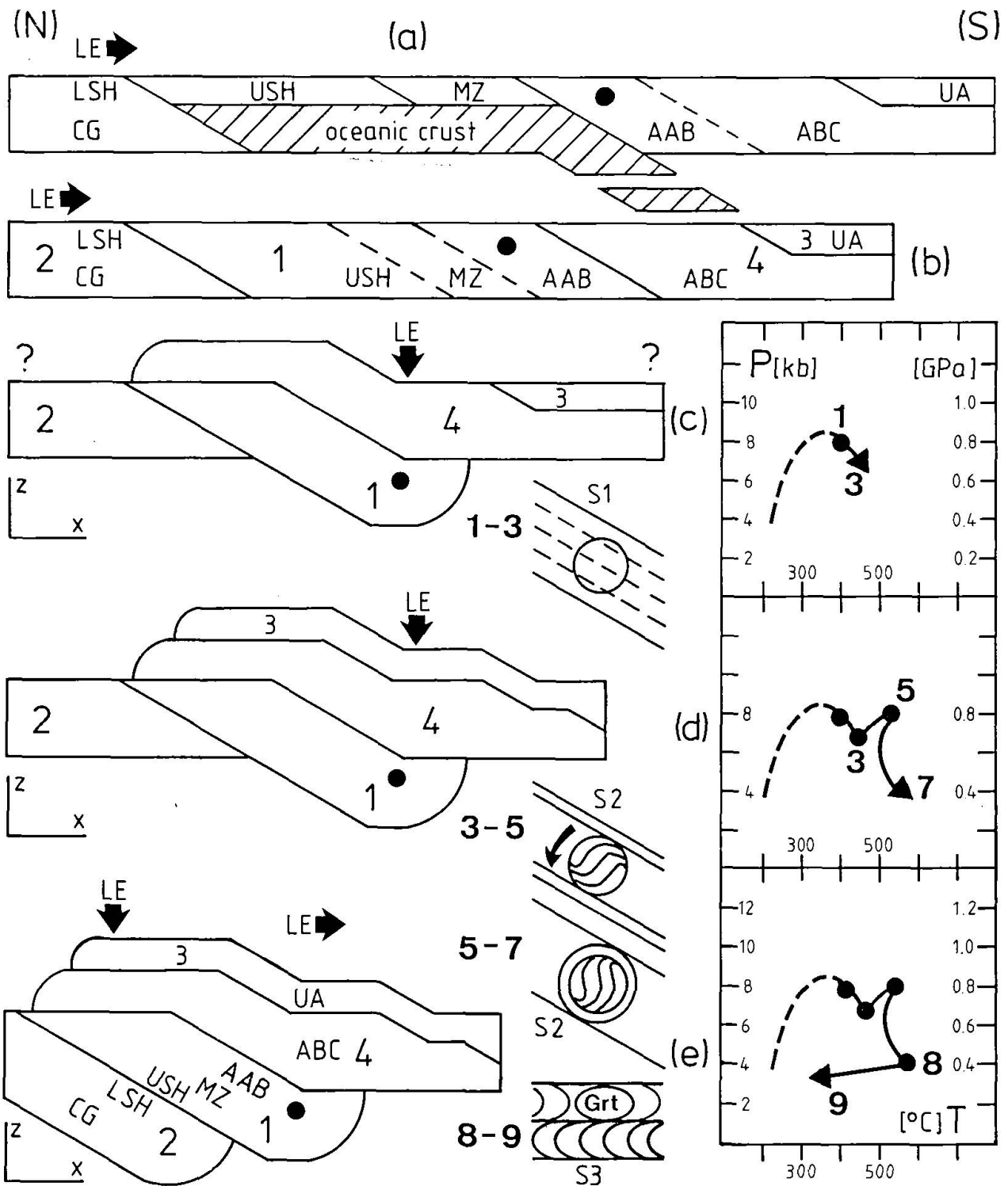


Fig. 6 Model of early-Alpine continental collision in the Eastern Alps. Successive stages of P-T evolution to the right refer to corresponding microstructures in the center and to a schematic tectonic evolution to the left. Bold numbers identify the steps of P-T evolution from Fig. 5b. AAB – Alpidic Austroalpine basement; ABC – Austroalpine basement complex; UA – Upper Austroalpine; MZ – Matreier Zone; LSH – autochthonous Lower Schieferhülle; USH – Upper Schieferhülle/allochthonous Lower Schieferhülle; CG – Central gneisses, LE – relative movement direction of level of erosion. (a) and (b) Situation previous to the collision, sampled area (point) is situated in the tectonic unit 1. (c) Underthrusting of unit 1 (USH, MZ, AAB) beneath the Adriatic Plate (ABC). Growth of garnet and corresponding HP-LT metamorphism (1–3) during subsequent isostatic uplift is shown to the right. (d) Overthrusting of unit 3 (UA) on the pre-existing pile. Resulting syncrystalline garnet rotation and re-increasing pressures (3–5) are followed by static garnet growth and uplift/heating (5–7). (e) Underthrusting of unit 2 (LSH, CG) causes an isobaric temperature-decrease (8–9) in unit 1, now belonging to the hangingwall, during generation of crenulation foliation S3 by predominant pure shear deformation S3. Note the relationship of X, Y, Z to the large-scale tectonic scenario.

Alpidic Austroalpine basement together with the Matreier Zone and the Upper Schieferhülle / allochthonous Lower Schieferhülle beneath the Adriatic (Apulian) Plate is the most important tectonic process. An overthrusting of a tectonic slab (probably the Upper Austroalpine unit) was additionally recorded. The time delay to a subsequent underthrusting of the Central Gneisses / allochthonous Lower Schieferhülle unit is responsible for a significant isobaric temperature-decrease in the garnet-micaschists. This tectonic scenario, derived by semiquantitative modelling of the shape of the relative P-T-t-deformation path provides additional information to previous ideas of other authors about the Alpine orogeny in the Eastern Alps (FRISCH, 1978; ROEDER and BÖGEL, 1978; TOLLMANN, 1987).

No clear interpretations of shear senses at the under- and overthrusting were possible from the existing structural data. However, a considerable simple shear deformation component with shearing perpendicular to Y is indicated by syncrystalline garnet rotation which was induced by an overthrusting event in course of D1-D2. Furthermore, the strain data signalizes substantial ductile shortening by a subsequent deformation D3 with a predominant pure shear deformation component. Such temporally changing types of deformation may be related to a changing of the relative tectonic position of the Alpidic Austroalpine basement in the collisional process. The subparallel orientation of the shearing direction during D1-D2 and the stretching lineation (D3) to the striking of the pre-collisional palaeogeographic zonation (TOLLMANN, 1987) implies an oblique collision between Adriatic and European plates.

Available radiometric geochronologic data suggests an early-Alpine age of the complete recorded thermotectonic history in the Alpidic Austroalpine basement. Discussions about middle- or late Alpine metamorphic and deformational events in the area refer to differential post-D3 cooling and uplift histories after the continental collision.

That way, tectonic modeling based on the shapes of P-T-t-deformation paths provides useful information and ideas to the understanding of orogenic processes.

#### Acknowledgements

The author is very grateful to Cl. Triboulet, CNRS Paris, and Cl. Audren, CNRS Rennes, for providing unpublished data and for their obliging help during research stays at Paris and Rennes. Microprobe analyses at Mineralogisches und Petrologisches Institut der Universität Bonn were assisted by B. Spiering. This paper was con-

troversially discussed with three reviewers. Their thorough comments improved the manuscript. J. Selverstone and J.E. Lieberman rejected the deformation/chemistry-related estimation of relative P-T variations, H. Abart expressed serious doubts about the validity of the applied method. The work was financed by a post-doctoral research grant from the Deutsche Forschungsgemeinschaft (DFG).

#### References

- BAGGIO, P., DALLA PORTA, A. and ZIRPOLI, G. (1971): Il complesso austroalpino di Cima Dura nella zona di Monte Spico (Alto Adige Orientale). *Studi Trentini Sc. Nat.*, 49, 3–31.
- BARNICK, H. (1965): Tektonische Untersuchungen in der westlichen Matreier Zone (Gebiet der Neuen Reichenberger Hütte, Ost-Tirol). *N. Jb. Geol. Paläont. Mh.*, 1965, 575–592.
- BEHRMANN, J.H. and WALLIS, S.R. (1987): Hangendverschuppung des Tauernfenster-Südrandes bei Kals (Osttirol) als Zeuge von eo-alpinem Underplating. *Jb. Geol. B.-A.*, 130/2, 133–138.
- BELL, T.H. (1985): Deformation partitioning and porphyroblast rotation in metamorphic rocks: a radical reinterpretation. *J. Metam. Geol.*, 3, 109–118.
- BELL, T.H. and JOHNSON, S.E. (1989): Porphyroblast inclusion trails: the key to orogenesis. *J. Metam. Geol.*, 7, 279–310.
- BLANCKENBURG, F.V., VILLA, I.M., BAUR, H., MORTEANI, G. and STEIGER, R.H. (1989): Time calibration of a P-T path from the Western Tauern Window, Eastern Alps: the problem of closure temperatures. *Contrib. Mineral. Petrol.*, 101, 1–11.
- BORSI, S., DEL MORO, A., SASSI, F.P., ZANFERRARI, A. and ZIRPOLI, G. (1978): New geopetrologic and radiometric data in the Alpine history of the Austridic continental margin south of the Tauern Window (Eastern Alps). *Mem. Ist. Geol. Min. Univ. Padova*, 32, 1–19.
- CIPRIANI, C., SASSI, F.P. and SCOLARI, A. (1971): Metamorphic white micas: definition of paragenetic fields. *Schweiz. Mineral. Petrogr. Mitt.*, 51, 259–302.
- CONTINI, R. and SASSI, F.P. (1980): Su alcuni effetti metamorfici Alpini nel basamento Austridico in Pusteria (Alpi Orientali). *Mem. Ist. Geol. Miner. Univ. Padova*, 34, 187–194.
- DAL PIAZ, G. (1934): Studi geologici sull'Alto Adige Orientale e regione limitrofe. *Mem. Ist. Geol. Univ. Padova*, 10, 238 p.
- DAVY, P. and GILLET, P. (1986): The stacking of thrust slices and its thermal consequences. *Tectonics*, 5, 913–929.
- DJRO, C., TRIBOULET, C. and AUDREN, C. (1980): Les chemins pression-température-temps-déformation-espace (P-T-t-d-e) dans les micaschistes associés aux schistes bleus de l'Ile de Groix. Bretagne Méridionale, France. *Schweiz. Mineral. Petrogr. Mitt.*, 69/1, 73–90.
- DROOP, G.T.R. (1985): Alpine metamorphism in the south-east Tauern Window, Austria: 1. P-T variations in space and time. *J. Metam. Geol.*, 3, 371–402.
- ENGLAND, P.C. and THOMPSON, A.B. (1984): Pressure-temperature-time paths of regional metamorphism 1. Heat transfer during the evolution of regions of thickened continental crust. *J. Petrol.*, 25, 894–928.
- ELLIS, M. and WATKINSON, A.J. (1987): Orogen-parallel extension and oblique tectonics: The relation be-

- tween stretching lineation and relative plate motions. *Geology*, 15, 1022–1026.
- FRANK, W., HÖCK, V. and MILLER, C. (1987): Metamorphic and tectonic history of the Central Tauern Window. In: FLÜGEL, H.W. and FAUPL, P. (Edit.) *Geodynamics of the Eastern Alps*, 34–54, Deuticke Verlag Wien.
- FRISCH, W. (1978): A plate tectonic model of the Eastern Alps. In: CLOSS, H., ROEDER, D. and SCHMIDT, K. (Edit.) *Alps, Apennines, Hellenides*. Inter-Union Commission on Geodynamics Scientific Report no. 38, 167–172, Schweizerbart Stuttgart.
- FRISCH, W., GOMMERINGER, K., KELM, U. and POPP, F. (1987): The Upper Bündner Schiefer of the Tauern Window – a key to understanding Eoalpine orogenic processes in the Eastern Alps. In: FLÜGEL, W. and FAUPL, P. (Edit.) *Geodynamics of the Eastern Alps*, 55–69, Deuticke Verlag Wien.
- GHENT, E.D. (1976): Plagioclase-garnet- $\text{Al}_2\text{SiO}_5$ -quartz: a potential geobarometer-geothermometer. *Am. Min.* 61, 710–714.
- GHENT, E.D. and STOUT, M.Z. (1981): Geobarometry and geothermometry of plagioclase-biotite-garnet-muscovite assemblages. *Contrib. Mineral. Petrol.*, 76, 92–97.
- GREEN, T.H. and HELLMAN, P.L. (1982): Fe–Mg partitioning between garnet and phengite at high pressure, and comments on a garnet-phengite geothermometer. *Lithos*, 15, 253–266.
- GREEN, N.L. and USDANSKY, S.I. (1986): Toward a practical plagioclase-muscovite thermometer. *Am. Min.*, 71, 1109–1117.
- GRUNDMANN, G. and MORTEANI, G. (1985): The young uplift and thermal history of the Central Eastern Alps (Austria/Italy), evidence from apatite fission track ages. *Jb. Geol. B.-A.*, 128, 197–216.
- HÖCK, V. (1980): Distribution maps of minerals of the Alpine metamorphism in the penninic Tauern Window, Austria. *Mitt. österr. geol. Ges.*, 71/72, 119–127.
- HÖCK, V. and HOSCHEK, G. (1980): Metamorphism of Mesozoic calcareous metasediments in the Hohe Tauern, Austria. *Mitt. österr. geol. Ges.*, 71/72, 99–118.
- HOERNES, S. and FRIEDRICHSEN, H. (1974): Oxygen isotope studies on metamorphic rocks of the western Hohe Tauern area (Austria). *Schweiz. Mineral. Petrogr. Mitt.*, 54, 769–788.
- HODGES, K.V. and SPEAR, F.S. (1982): Geothermometry, geobarometry and the  $\text{Al}_2\text{SiO}_5$  triple point at Mt. Moosilauke, New Hampshire. *Am. Min.*, 67, 1118–1134.
- HOFMANN, K.-H., KLEINSCHRODT, R., LIPPERT, R., MAGER, D. and STÖCKERT, B. (1983): Geologische Karte des Altkristallins südlich des Tauernfensters zwischen Pfunderer Tal und Tauferer Tal (Südtirol). *Der Schlern*, 53, 572–590.
- HOLDAWAY, M.J. and LEE, S.M. (1977): Fe–Mg cordierite stability in high-grade pelitic rocks based on experimental, theoretical and natural observations. *Contrib. Mineral. Petrol.*, 63, 175–198.
- JÄGER, E. (1979): Introduction to Geochronology. In: JÄGER, E. and HUNZIKER, J.C. (Edit.) *Lectures in isotope geology*, 1–12, Springer Verlag Berlin.
- KLEINSCHRODT, R. (1987): Quarzkorngefüge im Altkristallin südlich des westlichen Tauernfensters (Südtirol/Italien). *Erlanger geol. Abh.*, 114, 1–82.
- LAMMERER, B. (1988): Thrust regime and transpression-regime tectonics in the Tauern Window (Eastern Alps). *Geol. Rdsch.*, 77, 143–156.
- MASSONNE, H.-J. and SCHREYER, W. (1987): Phengite geobarometry based on the limiting assemblage with K-feldspar, phlogopite and quartz. *Contrib. Mineral. Petrol.*, 96, 212–224.
- MASUDA, T. and MOCHIZUKI, S. (1989): Development of snowball structure: numerical simulation of inclusion trails during synkinematic porphyroblast growth. *Tectonophysics*, 170/1, 141–150.
- MARTIGNOLE, J. and NANTEL, S. (1982): Geothermobarometry of cordierite-bearing metapelites near the Morin anorthosite complex, Grenville province, Quebec. *Canadian Mineral.*, 20, 307–318.
- NEWTON, R.C. and HASELTON, H.T. (1981): Thermodynamics of the garnet-plagioclase- $\text{Al}_2\text{SiO}_5$ -quartz geobarometer. In: NEWTON, R.C., NAVROTSKY, A. and WOOD, B.J. (Edit.) *Thermodynamics of minerals and melts*, 131–147, Springer Verlag New York.
- NOLLAU, G. (1969): Kleintektonische Strukturen am SW-Rand des Tauernfensters und ihre Einbeziehung in grobstektonische Konzepte. *Geol. Rdsch.*, 58, 755–788.
- OXBURGH, E.R. and ENGLAND, P.C. (1980): Heat flow and the metamorphic evolution of the Alps. *Eclogae geol. Helv.*, 73, 379–398.
- OXBURGH, E.R. and TURCOTTE, D.L. (1974): Thermal gradients and regional metamorphism in overthrust terrains with special reference to the Eastern Alps. *Schweiz. Mineral. Petrogr. Mitt.*, 54, 641–662.
- PERCHUK, L.L. and ARANOVITCH, L.Y. (1984): Improvement of biotite-garnet geothermometer: correction for fluorine content in biotite. *Dokl. Acad. Sci. USSR*, 277, 471–475.
- POWELL, D. and TREAGUS, J.E. (1969): On the geometry of S-shaped inclusion trails in garnet porphyroblasts. *Mineral. Mag.*, 36, 453–456.
- PROCHASKA, W. (1981): Einige Ganggesteine der Rieserfernerintrusion mit neuen radiometrischen Altersdaten. *Mitt. Ges. Geol. Bergbaustud. Österr.*, 27, 161–171.
- RAASE, P. and MORTEANI, G. (1976): The potassic feldspar in metamorphic rocks of the western Hohe Tauern area, Eastern Alps. *Geol. Rdsch.*, 65, 422–436.
- RAITH, M., RAASE, D., KREUZER, H. and MÜLLER, D. (1978): The age of the Alpidic metamorphism in the western Tauern Window, Austrian Alps, according to radiometric dating. In: CLOSS, H., ROEDER, D.H. and SCHMIDT, K. (Edit.) *Alps, Apennines, Hellenides*. Inter-Union Commission on Geodynamics Scientific Report No. 38, 140–148, Schweizerbart Stuttgart.
- RAMSAY, J.G. and HUBER, M.I. (1983): The techniques of modern structural geology. Volume 1: Strain analysis, 307 p., Academic Press London.
- ROEDER, D. and BÖGEL, H. (1978): Geodynamic interpretation of the Alps. In: CLOSS, H., ROEDER, D.H. and SCHMIDT, K. (Edit.) *Alps, Apennines, Hellenides*. Inter-Union Commission on Geodynamics Scientific Report No. 38, 191–212, Schweizerbart Stuttgart.
- SANDER, B. (1921): Geologische Studien am Westende der Hohen Tauern (2. Bericht). *Jb. Geol. R.-A. Wien*, 70, 273–296.
- SASSI, F.P., ZANFERRARI, A., ZIRPOLI, G., BORSI, S. and DEL MORO, A. (1974): The Austrides to the south of the Tauern Window and the Periadriatic Lineament between Mules and Mauthen. *N. Jb. Geol. Paläont. Mh.*, 1974, 421–434.
- SASSI, F.P., BELLINI, G., PECCERILLO, A. and POLI, G. (1980): Some constraints on geodynamic models in the Eastern Alps. *N. Jb. Geol. Paläont. Mh.*, 1980/9, 541–548.
- SATIR, M. and FRIEDRICHSEN, H. (1986): Geochronologi-

- cal and stable isotope investigations on polymetamorphic rocks from the Eastern Alps (Western Tauern Window, Austria). *N. Jb. Mineral.*, 154, 313–334.
- SCHONEVELD, C. (1977): A study of some typical inclusion patterns in strongly paracrystalline-rotated garnets. *Tectonophysics*, 39, 453–471.
- SELVERSTONE, J. (1988): Evidence for east-west crustal extension in the Eastern Alps: implications for the unroofing history of the Tauern Window. *Tectonics*, 7, 87–105.
- SELVERSTONE, J. and SPEAR, F.S. (1985): Metamorphic P-T paths from pelitic schists and greenstones from the southwest Tauern Window, Eastern Alps. *J. Metam. Geol.*, 3, 439–465.
- SELVERSTONE, J., SPEAR, F.S., FRANZ, G. and MORTEANI, G. (1984): High-pressure metamorphism in the SW Tauern Window, Austria: P-T paths from hornblende-kyanite-staurolite schists. *J. Petrol.*, 25, 501–531.
- SENARCLENS-GRANCY, W. (1972): Geologische Karte der westlichen Deferegger Alpen 1 : 25 000. Geologische Bundesanstalt Österreich (Edit.), Wien.
- SPEAR, F.S. and RUMBLE, D. (1986): Pressure, temperature and structural evolution of the Orfordville Belt, West-Central New Hampshire. *J. Petrol.*, 27, 1071–1093.
- SPEAR, F.S. and SELVERSTONE, J. (1983): Quantitative P-T paths from zoned minerals: theory and tectonic applications. *Contrib. Mineral. Petrol.*, 83, 348–357.
- SPEAR, F.S., SELVERSTONE, J., HICKMOTT, D., CROWLEY, P. and HODGES, K.V. (1984): P-T paths from garnet zoning: a new technique for deciphering tectonic processes in crystalline terranes. *Geology*, 12, 87–90.
- STÖCKHERT, B. (1982): Deformation und retrograde Metamorphose im Altkristallin südlich des westlichen Tauernfensters (Südtirol). Diss. Universität Erlangen-Nürnberg, Veröff. Geol. Inst. Erlangen, 1982/2, 1–230.
- STÖCKHERT, B. (1984): K-Ar determinations on muscovites and phengites from deformed pegmatites, and the minimum age of the Old Alpine deformation in the Austriac basement south of the western Tauern Window (Ahrn valley, Southern Tyrol, Eastern Alps). *N. Jb. Min. Abh.*, 150, 103–120.
- STÖCKHERT, B. (1985): Pre-Alpine history of the Austriac basement to the south of the western Tauern Window (Southern Tyrol, Italy) – Caledonian versus Hercynian event. *N. Jb. Geol. Paläont. Mh.*, 1985/10, 618–842.
- THOMPSON, A.B. (1976): Mineral reactions in pelitic rocks. *Am. J. Sci.*, 276, 401–454.
- THOMPSON, A.B. and ENGLAND, P.C. (1984): Pressure-temperature-time paths of regional metamorphism, II: their inference and interpretation using mineral assemblages in metamorphic rocks. *J. Petrol.*, 25, 929–955.
- TOLLMANN, A. (1987): Neue Wege in der Ostalpengeologie und die Beziehungen zum Ostmediterrän. *Mitt. österr. geol. Ges.*, 80, 47–113.
- TRACY, R.J. (1982): Compositional zoning and inclusions in metamorphic minerals. In: FERRY, J.M. (Edit.) *Characterization of metamorphism through mineral equilibria*. Mineral. Soc. Am. Rev. in Mineral. 10, 355–397.
- TRIBOULET, C. and AUDREN, C. (1985): Continuous reactions between biotite, garnet, staurolite, kyanite-sillimanite-andalusite and P-T-time-deformation path in micaschists from the estuary of the river Vilaine, South Brittany, France. *J. Metam. Geol.*, 3, 91–105.
- TRIBOULET, C. and AUDREN, C. (1988): Controls on P-T-t-deformation path from amphibole zonation during progressive metamorphism of basic rocks (estuary of the River Vilaine, South Brittany, France). *J. Metam. Geol.*, 6, 117–133.
- TRZCIENSKI, W.E. (1977): Garnet zoning – product of a continuous reaction. *Canadian Mineral.*, 15, 250–256.
- VELDE, B. (1967): Si<sup>4+</sup> contents of natural phengites. *Contrib. Mineral. Petrol.*, 14, 250–258.
- ZARSKÉ, G. (1985): Kartierung, Strukturgeologie und Petrographie im Altkristallin zwischen Erlsbach und Oberseitsee in den nordwestlichen Deferegger Alpen, Osttirol. Unpublished Diploma Thesis, Institut für Geologie und Paläontologie, Techn. Univ. Clausthal, 178 p.

Manuscript received February 5, 1990; revised manuscript accepted August 13, 1990.